Dual-gate low voltage organic transistor for pressure sensing

Yushi Tsuji[1], Heisuke Sakai[1], Linrun Feng[2], Xiaojun Guo[2] and Hideyuki Murata[1*]

[1]School of Materials Science, Japan Advanced Institute of Science and Technology, 1-1 Asahidai, Nomi, Ishikawa 923-1292, Japan

[2]National Engineering Laboratory for TFT-LCD Material and Technologies, Department of Electronic Engineering, Shanghai Jiao Tong University, Shanghai 200240, China

*E-mail: murata-h@jaist.ac.jp

Abstract

We simultaneously achieved low voltage operation (-5 V) and large drain current (I_D) modulation in a dual-gate organic pressure sensor in which a piezoelectric layer was stacked on a low voltage organic field-effect transistor (OFET). During testing, the I_D changed from 3.9×10^{-9} A to 2.5×10^{-11} A when a 300 kPa pressure load was applied, and the I_D clearly responded to the pressure load and release. An endurance cycle test of the device was performed using a pressure load of 100 kPa, and the I_D modulation was consistently reproduced throughout the test.

Recently, organic pressure sensors have been actively studied in anticipation of their application in the health care field, in areas such as artificial skin, human pulse measurement systems, sensors for the detection of bedsores, and sensor sheets for floors.[1-4] In these applications, the flexibility of the sensors has been one of the key requirements in order to detect biological information associated with the human body. As a result, organic pressure sensors are promising candidates for these applications because of their state-of-the-art intrinsic flexibility. The high degree of compatibility between organic pressure sensors and low-cost printing processes also makes them suitable for large-area sensing arrays. Of all the methods that can be used to construct these devices,[2,5-9] one efficient method employs a pressure sensor composed of a capacitor or a resistor as a sensing device and an organic field-effect transistor (OFET) as a readout device. The pressure sensor responds to changes in the pressure load on the sensing device by changing the drain current (I_D) of the OFET.[10-12] In this case, the sensor has several advantages, including a high sensitivity to the pressure load and less susceptibility to crosstalk in a circuit. In the past, a large area pressure sensor sheet was developed that incorporated hundreds of transistors and had a sensing area of 80 mm by 80 mm.[13] By employing an OFET with a suspended gate, Zhang et al. achieved a large modulation of the I_D of the OFET that was more than three orders of magnitude under a pressure load of approximately 1.2 kPa.[14] However, the reported high operating voltage (40–60 V) of these sensors prevents them from being used in practical applications. Consequently, it is important to reduce the operating voltage of these devices. Because the sensing capacitor and

readout OFET are functionally separated in the pressure sensor, one key for further improvements in device performance has been to employ a new device architecture based on the concept of functional separation. Lai *et al*. have achieved the low voltage (-2 V) operation of an organic pressure sensor in which the OFET and a sensing capacitor composed of polydimethylsiloxane (PDMS) film were developed separately, and then integrated using a floating gate electrode.[15] Although low voltage operation has been achieved, the relative change in the drain current ($\Delta I/I_{min}$) versus the pressure load (78 kPa) was only approximately 0.04, where ΔI is the change in I_D under pressure load and I_{min} is the minimum value of I_D under the pressure load test. This small change in I_D suggests that the change in the capacitance of the sensing capacitor based on the pressure load would be too small to modulate the I_D in an integrated OFET. Recently, we reported a pressure sensor with a $\Delta I/I_{min}$ of 23 for a pressure load of 100 kPa at a low operating voltage of -6 V.[16] A polarized copolymer of vinylidene fluoride (VDF) and trifluoroethylene (TrFE) with a VDF to TrFE ratio of 75:25 [P(VDF-TrFE)] was employed as the dielectric of the sensing capacitor, which was then integrated as the readout device of a low voltage OFET to complete the device fabrication process. The $\Delta I/I_{min}$ value of 23 was over 500 times larger than that for the previously mentioned low voltage organic pressure sensor in which $\Delta I/I_{min} = 0.04$.[15] The higher $\Delta I/I_{min}$ was due to the polarization of the P(VDF-TrFE) layer. These results indicate that the I_D modulation in the low voltage OFET in the sensing capacitor is a promising approach to achieve a low voltage organic pressure sensor. In this paper, we present a dual-gate organic pressure sensor, where the sensing

capacitor in the piezoelectric layer is stacked on top of the readout low voltage OFET (referred to as a dual-gate organic pressure sensor). Because the top and bottom gates are functionally and electrically separated, we can independently develop and control both the capacitor and OFET in order to maximize the performance as a pressure sensing device. Consequently, a $\Delta I/I_{min}$ of 155 versus a pressure load of 300 kPa at a low operating voltage of -5 V was achieved. In addition, the clear response of the I_D to the application and release of the pressure load was observed, and the endurance cycle test of the device versus the pressure load of 100 kPa demonstrated that the I_D modulation was reproducible.

Figure 1 shows the schematic structure of the dual-gate organic pressure sensor, in which the active and dielectric layers are located between top and bottom gate electrodes, as is the case in other conventional dual-gate transistors.[17-19] The sensing capacitor and the low voltage OFET of the dual-gate organic pressure sensor were developed separately. During fabrication of the OFET, a 30 nm Al bottom gate electrode was thermally evaporated onto a glass substrate. The 300 nm thick Poly(vinyl cinamate) (PVC) gate dielectric layer was spin-coated and cross-linked by UV irradiation. The UV-photocrosslinking was confirmed using a Fourier-transform infrared (FT-IR) measurement, as previously reported.[16,20] The 50 nm Ag source/drain electrodes were thermally evaporated and modified by immersion in a solution of Pentafluorothiophenol in ethanol. The channel width and length were 2 mm and 50 μm, respectively. The 100 nm thick semiconductor layer was spin-coated from a mixed solution of 6,13-bis(triisopropyl-silylethynyl)pentacene

(TIPS-Pentacene) and Polystyrene (PS).[21] This approach to obtain the low-voltage OFET can be applied for the plastic substrate,[22] and our sensor on the plastic substrate would be reported elsewhere. As the piezoelectric layer of the sensing capacitor, the P(VDF-TrFE) layer was blade-coated onto an n-type high-doped Si substrate followed by the contact poling of P(VDF-TrFE) with a poling condition of 1 kV to an electrode. The change in the orientation of the P(VDF-TrFE) chain was confirmed by an FT-IR measurement of the film.[16] The FT-IR absorption spectra were measured with a Thermo Nicolet 6700 FT-IR spectrometer. The resolution of the spectra was 4 cm^{-1}, and the number of scans collected was 128. The P(VDF-TrFE) piezoelectric layer with the Si substrate as the top electrode was then stacked on top of the OFET. The top electrode was grounded during the pressure application on the device. The electrical properties of the OFET were characterized using a Keithley 4200 semiconductor characterization system. The pressure response of the sensor device was evaluated as the change in I_D of the OFET in response to the pressure load on the piezoelectric layer applied with a homemade pressure load system. All electrical measurements were performed at 25 °C in a dry nitrogen atmosphere.

In this case, the I_D of the OFET can be independently controlled by each gate since the gate electrodes are electrically isolated by the gate dielectric. For example, the transfer curve representing the application of voltage from the bottom gate electrode (V_{Gbot}) can be shifted by the application of voltage from the top gate electrode (V_{Gtop}), and the magnitude of the shift is proportional to V_{Gtop}.[18,19] As shown in Figs. 1(a) and 1(b), we stacked a polarized P(VDF-TrFE)

piezoelectric layer with an electrode on top of the active layer, which then shifted the transfer curve of the OFET. That is, the surface potential of the polarized P(VDF-TrFE) layer at the interface between the active layer and the P(VDF-TrFE) layer changes as a pressure load is applied to the piezoelectric layer due to the piezoelectric characteristics of the P(VDF-TrFE). This change in the surface potential corresponds to the change in the V_{Gtop} in conventional dual-gate OFETs. Thus, the transfer curve can be shifted by applying pressure to the P(VDF-TrFE) piezoelectric layer. Consequently, the I_D of the dual-gate organic pressure sensor at a particular V_{Gbot} changes according to the pressure load on the device. In addition, the change in the I_D due to the change in the polarization of the P(VDF-TrFE) layer remains constant since the change in surface potential under a particular pressure load is constant. As a result, a high reproducibility of the I_D modulation of the organic pressure sensor to a certain pressure load is expected.

Figure 2(a) shows the IR spectra of P(VDF-TrFE) film before (pristine) and after (polarized) the contact poling treatment. As the CF_2 group is oriented by the contact poling treatment of the film, the change in the FT-IR spectra of the P(VDF-TrFE) film after poling treatment corresponds to the change in the rotation of the polymer chain.[23] And, FT-IR measurement of the film is effective to reveal the molecular orientation of the polymer, and thus the assignment of each bands is essential.[24] The band at 1290 cm^{-1} is assigned to C-C stretching. The band at 1180 cm^{-1} is assigned to CF_2 antisymmetric stretching. The band at 883 cm^{-1} is assigned to CH_2 rocking. The band at 844 cm^{-1} is assigned to CF_2 symmetric stretching. As shown in the difference spectrum of the film (Fig.

2(b)), the intensities of the bands observed at 1290 and 844 cm^{-1} decrease after the polarization. As the transition dipole moment of the bands is parallel to the permanent dipole moment of the CF_2 group, the decrease in the absorbance corresponds to the rotation of CF_2 group toward the surface normal in average. The intensities of the bands observed at 1180 and 883 cm^{-1} increase after the polarization since the transition dipole moment of the bands are perpendicular to the permanent dipole moment of the CF_2 group, which is attributed to the change in the tilt of the polymer chain parallel to the surface. In other words, the CF_2 group tilts toward the surface normal. These results are consistent with the other paper.[24] Based on these results, we confirmed the P(VDF-TrFE) film were polarized by the contact poling treatment.

Figure 3(a) shows the output characteristics of the OFET. The drain voltage (V_D) was swept from 0 V to -5 V in steps of 0.1 V, and the gate voltage (V_G) was swept from 0 V to -5 V in steps of 1 V. In the transfer characteristic measurement shown in Fig. 3(b), the V_G was swept from 1 V to -5 V with a step voltage of 0.1 V at a V_D of -5 V. The ON/OFF ratio, mobility, threshold voltage (V_{TH}), and subthreshold swing value were calculated to be 5.1×10^4, 0.27 cm^2/Vs, -0.8 V, and 310 mV/dec, respectively. Based on these results, it is clear that the OFET operated properly at a low operating voltage.

Figure 4(a) shows the changes in the transfer characteristics of the OFET at V_D = -5 V, which were measured before (denoted as Initial in the figure) and after (denoted as 0 kPa) the piezoelectric layer was integrated into the OFET and the pressure loads were applied to the device (denoted as

100, 200, 300, and 400 kPa). When the P(VDF-TrFE) piezoelectric layer was stacked onto the OFET, the transfer characteristics shifted from their initial position (V_{TH} = -1.1 V) to the 0 kPa position (V_{TH} = -1.5 V). Based on the operating mechanism of the conventional dual-gate OFET, this shift corresponded to the application of the positive bias from the top electrode ($V_{Gtop} > 0$).[17-19] In our case, the polarization of the P(VDF-TrFE) piezoelectric layer caused a positive bias to be applied to the device. Consequently, the P(VDF-TrFE) layer polarized with a poling condition at 1 kV caused a negative shift of the transfer curve. In contrast, the direction of the shift caused by the stacking of the P(VDF-TrFE) piezoelectric layer was opposite to the shift when we stacked a P(VDF-TrFE) layer polarized with a poling condition at -1 kV. Furthermore, the shift was not observed when a non-polarized P(VDF-TrFE) layer was stacked (Fig.4(b)). These shifts in the transfer curve that were induced by the polarized dielectric are consistent with the results of our previous study.[16] Therefore, we concluded that the shift of the transfer curve was induced by the polarization of the P(VDF-TrFE) piezoelectric layer.

In order to clarify the pressure response of the I_D, 0 kPa to 400 kPa of pressure was applied to the device in steps of 100 kPa, as shown in Fig. 4(a), and the transfer characteristics shifted in response to the pressure load. In our device, the surface of the polarized P(VDF-TrFE) piezoelectric layer was positively charged. After the integration of the piezoelectric layer, the surface potential of the positive charge was enhanced by the piezoelectric characteristics when pressure was applied to the P(VDF-TrFE) piezoelectric layer. This enhancement of the surface potential corresponds to the

application of the V_{Gtop} in the case of conventional dual-gate OFETs. Consequently, the transfer characteristics shifted in steps as the pressure load was increased from 0 kPa to 400 kPa. In order to further investigate the pressure induced shift of the transfer curve, we prepared a dual-gate pressure sensor with a non-polarized P(VDF-TrFE) layer, and the shift was not observed in this device when pressure was applied. In addition, when we stacked a P(VDF-TrFE) layer whose direction of polarization was opposite to that in the case of the pressure sensor in Fig. 4(a), the shift was observed in the opposite direction. Thus, we concluded that the shifts of the transfer curve in Fig. 4(a) were due to the pressure load on the polarized P(VDF-TrFE) layer.

Figure 4(c) shows the I_D response of the OFET at V_{Gbot} = -1.8 V. The pressure load was incrementally applied to the device from 0 kPa to 300 kPa in steps of 100 kPa followed by the controlled release of the pressure load. Each pressure load was maintained for approximately 40 s to confirm the stability of the I_D under the pressure load. As can be seen, the I_D values at each pressure load decrease as the value of the pressure load increases, which is consistent with the decrease in I_D at V_{Gbot} = -1.8 V as function of the pressure load in Fig. 4(a). The I_D decreased from 3.9×10^{-9} A to 2.5×10^{-11} A as the pressure load changed from 0 kPa to 300 kPa. The $\Delta I/I_{min}$ value of 155 was over three orders of magnitude larger than that for the other low voltage organic pressure sensor in which $\Delta I/I_{min}$ = 0.04.[15] A linear relationship between log I_D as a function of the pressure load at V_{Gbot} = -1.8 V was observed (refer to the inset of Fig. 4(c)), where a pressure induced I_D modulation of 139 kPa/dec was achieved. These features of the pressure device are due to the dual-gate structure. That

is, the value of the $\Delta I/I_{min}$ can be tuned to a maximum value by applying an appropriate V_{Gbot} to the OFET, since the ΔI and the I_{min} are tuned as a function of V_{Gbot}. In the case of Fig. 4(c), we applied V_{Gbot} = -1.8 V during the operation to obtain the maximum value of the $\Delta I/I_{min}$, which is in the subthreshold region of the OFETs. As a result of the small value of the subthreshold swing (i.e. 310 mV/dec) and the measurement of the I_D in the subthreshold region of the OFETs, the change in the I_D at a certain V_{Gbot} based on the shift of the transfer curve due to the pressure load became large. We therefore achieved a larger $\Delta I/I_{min}$ by applying the pressure load.

To confirm the reproducibility of the change in I_D values under constant pressure loads, an endurance cycle test of the device versus the pressure load (100 kPa) was carried out (Fig. 4(d)) and the I_D was observed to decrease from 3.9×10^{-9} A to 7.0×10^{-10} A when the pressure load was applied, and returned to the initial value when the pressure was released. The relationship between the I_D value and the pressure load was found to be repeatable. From these results, it was clear that the I_D responded to the pressure load and release. Furthermore, the endurance cycle test of the device versus the pressure load demonstrated that the observed I_D modulation was repeatable.

In conclusion, we have simultaneously achieved low voltage operation (-5 V) and high modulation of I_D in a dual-gate organic pressure sensor, in which a piezoelectric layer was stacked on a low voltage OFET. The I_D changed from 3.9×10^{-9}A to 2.5×10^{-11}A when a pressure load of 300 kPa was applied, as shown in Fig. 4(c). A $\Delta I/I_{min}$ value of 155 and a pressure induced I_D modulation of 139 kPa/dec at V_{Gbot} of -1.8 V and V_D of -5 V were obtained. In addition, a clear response of the

I_D to the application and release of the pressure load was observed. Furthermore, the endurance cycle test of the device versus the pressure load demonstrated that the I_D modulation was reproducible. And the fabrication of the dual-gate architecture composed of the sensing capacitor and OFET would be compatible for the lamination technique or the roll-to-roll technique for development of the large scale and high resolution pressure sensing sheet. Based on these results, this dual-gate organic pressure sensor holds great potential for applications in health monitoring and robotics.

Acknowledgement

The work was supported by Grants-in-Aid (16K21061 to H.S.) from the Ministry of Education, Culture, Sports, Science, and Technology (MEXT).

Figure Captions

Fig. 1 (Color online) (a) The schematic structure of the dual-gate organic pressure sensor. (b) Image of the dual-gate low voltage organic transistors. Low-voltage transistors are fabricated on the glass substrate followed by integration of P(VDF-TrFE)/Si substrate.

Fig. 2 (Color online) (a) FT-IR spectra of P(VDF-TrFE) film before (pristine) and after (polarized) the contact poling treatment. (b) The polarization induced IR difference spectrum of the film. The difference spectrum was obtained by subtracting the spectra of the pristine film from the spectra of the polarized film.

Fig. 3 (Color online) (a) The output characteristics of the OFET. (b) The transfer characteristics of the OFET.

Fig. 4 (Color online) (a) The shifts of transfer curve of the OFET corresponding to the pressure load. (b) The transfer curves of the OFET before and after integration of the non-polarized P(VDF-TrFE) layer. (c) The I_D response of the OFET at V_{Gbot} = -1.8 V. The pressure load was incrementally applied onto the device from 0 kPa to 300 kPa with a step pressure load of 100 kPa. The log I_D as a function of the pressure load at V_{Gbot} = -1.8 V is shown in the inset. (d) The endurance cycle test of the device against the pressure load (100 kPa).

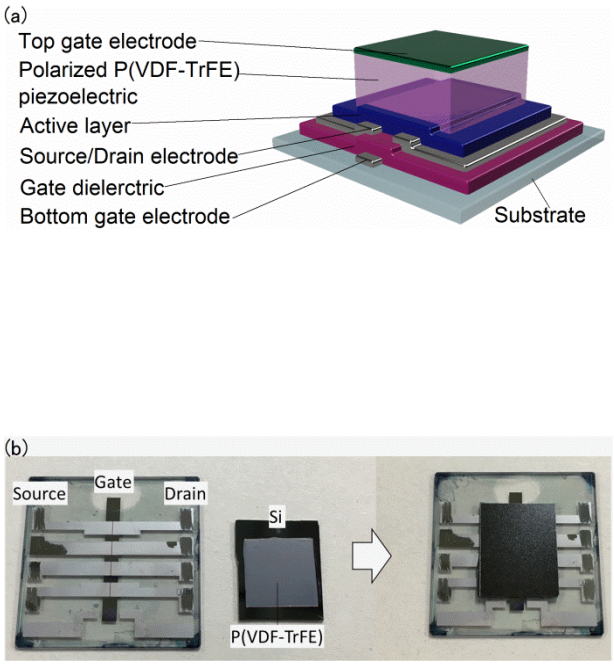

Fig.1
Y. Tsuji et al. APEX

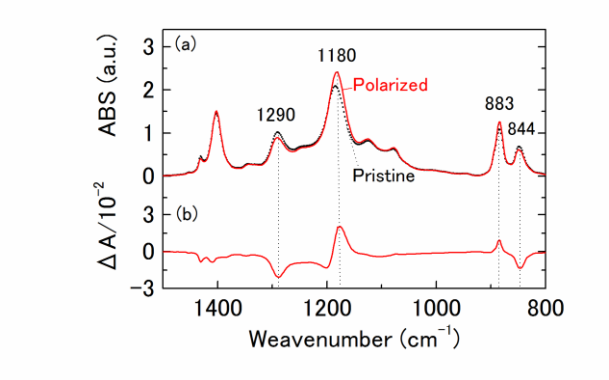

Fig.2
Y. Tsuji et al. APEX

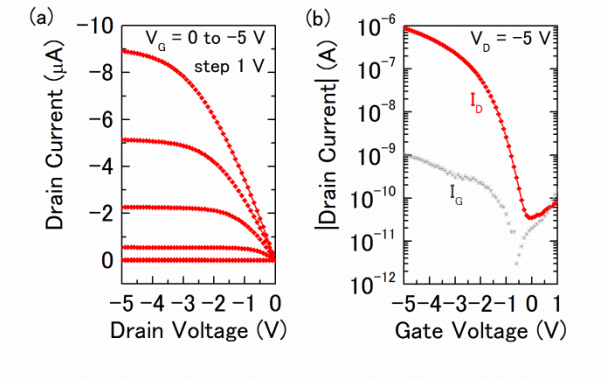

Fig.3
Y. Tsuji et al. APEX

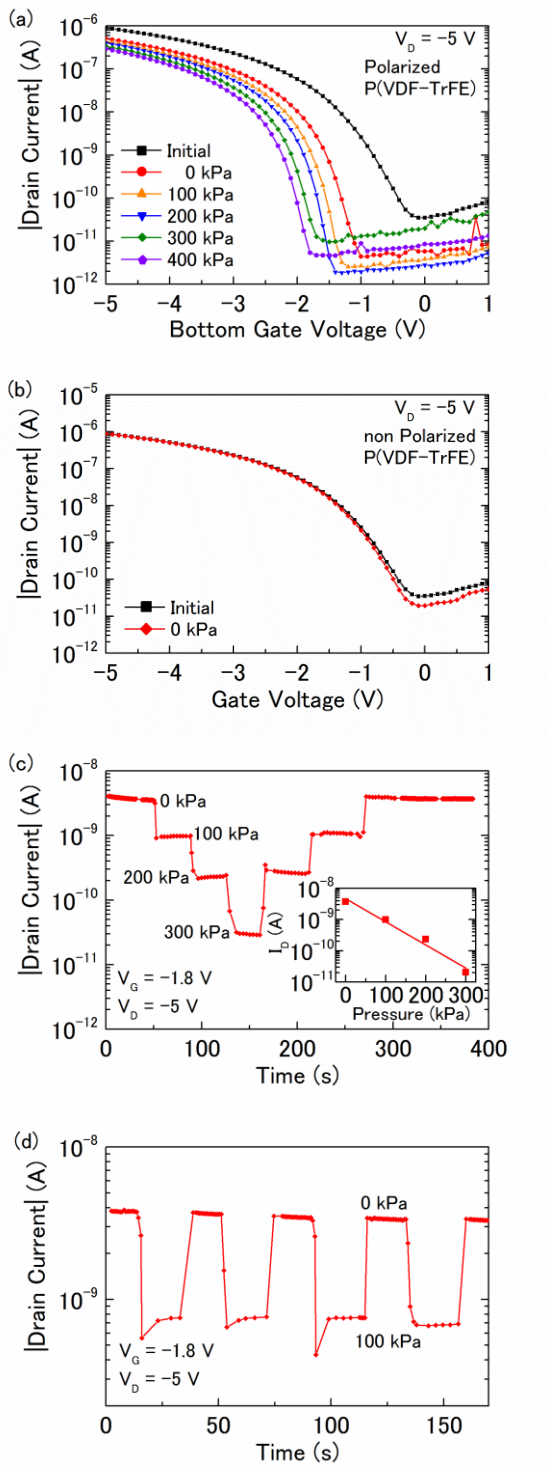

Fig.4

Y. Tsuji et al. APEX

References

1) C.-L. Choong, M.-B. Shim, B.-S. Lee, S. Jeon, D.-S. Ko, T.-H. Kang, J. Bae, S. H. Lee, K.-E. Byun, J. Im, Y. J. Jeong, C. E. Park, J.-J. Park, and U. I. Chung: Adv. Mater. **26** (2014) 3451.
2) G. Schwartz, B. C. K. Tee, J. Mei, A. L. Appleton, D. H. Kim, H. Wang, and Z. Bao: Nature Communications **4** (2013) 1859.
3) T. Q. Trung and N.-E. Lee: Adv. Mater. **28** (2016) 4338.
4) S. Uemura, Y. Watanabe, M. Yoshida, H. Tokuhisa, and N. Takada: J. Photopolym. Sci. Technol. **26** (2013) 411.
5) K. F. Lei, K.-F. Lee, and M.-Y. Lee: Microelectron. Eng. **99** (2012) 1.
6) H. Mei, R. Wang, Z. Wang, J. Feng, Y. Xia, and T. Zhang: Sensors and Actuators A: Physical **222** (2015) 80.
7) Q. Sun, D. H. Kim, S. S. Park, N. Y. Lee, Y. Zhang, J. H. Lee, K. Cho, and J. H. Cho: Adv. Mater. **26** (2014) 4735.
8) Z. Wang, S. Wang, J. Zeng, X. Ren, A. J. Y. Chee, B. Y. S. Yiu, W. C. Chung, Y. Yang, A. C. H. Yu, R. C. Roberts, A. C. O. Tsang, K. W. Chow, and P. K. L. Chan: Small **12** (2016) 3827.
9) Y. Watanabe, S. Uemura, and S. Hoshino: Jpn. J. Appl. Phys. **53** (2014) 05HB15.
10) J. Kim, T. Nga Ng, and W. Soo Kim: Appl. Phys. Lett. **101** (2012) 103308.
11) S. Lai, P. Cosseddu, A. Bonfiglio, and M. Barbaro: IEEE Electron Device Letters **34** (2013) 801.
12) S. C. B. Mannsfeld, B. C. K. Tee, R. M. Stoltenberg, C. V. H. H. Chen, S. Barman, B. V. O. Muir, A. N. Sokolov, C. Reese, and Z. Bao: Nat Mater **9** (2010) 859.
13) T. Someya, T. Sekitani, S. Iba, Y. Kato, H. Kawaguchi, and T. Sakurai: Proc. Natl. Acad. Sci. U. S. A. **101** (2004) 9966.
14) Y. Zang, F. Zhang, D. Huang, X. Gao, C.-a. Di, and D. Zhu: Nat Commun **6** (2015) 6269.
15) S. Lai, P. Cosseddu, A. Bonfiglio, and M. Barbaro: Electron Device Letters, IEEE **34** (2013) 801.
16) H. Sakai, Y. Tsuji, and H. Murata: IEICE Transactions (Accepted).
17) S. Iba, T. Sekitani, Y. Kato, T. Someya, H. Kawaguchi, M. Takamiya, T. Sakurai, and S. Takagi: Appl. Phys. Lett. **87** (2005) 023509.
18) J. B. Koo, C. H. Ku, J. W. Lim, and S. H. Kim: Org. Electron. **8** (2007) 552.
19) F. Maddalena, M. Spijkman, J. J. Brondijk, P. Fonteijn, F. Brouwer, J. C. Hummelen, D. M. de Leeuw, P. W. M. Blom, and B. de Boer: Org. Electron. **9** (2008) 839.
20) L. Feng, H. Sakai, Y. Sakuragawa, R. Wang, J. Zhao, H. Murata, and X. Guo: Org. Electron. **26** (2015) 471.
21) L. Feng, W. Tang, X. Xu, Q. Cui, and X. Guo: Electron Device Letters, IEEE **34** (2013) 129.
22) L. Feng, W. Tang, J. Zhao, Q. Cui, C. Jiang and X. Guo: Trans Electron Devices, IEEE **61** (2014) 2014.
23) X. Ma, J. Liu, C. Ni, D. C. Martin, D. B. Chase and J. F. Rabolt: ACS Macro Letters, **1** (2012) 428.
24) H. Isoda and Y. Furukawa: Vib. Spectrosc, **78** (2015)12.